3 MECHANICAL PROPERTY CHARACTERISATION OF PLANT YARN REINFORCED THERMOSET MATRIX COMPOSITES*

3.1 Introduction

Employing plant fibre yarns as continuous reinforcements for unidirectional composites, this chapter evaluates the mechanical properties of aligned plant fibre composites (PFRPs), against aligned E-glass composites (GFRPs), to appreciate the true potential of biofibres as stiffness-inducing reinforcements. As composite materials are heterogeneous, the reinforcement and matrix type will obviously affect composite properties. Noting the effectiveness of aligned bast fibre reinforcements (e.g. flax, hemp and jute) and thermoset matrices (e.g. unsaturated polyester and epoxy) for load-bearing composites (as highlighted in *Chapter 2*), this study examines the effect of plant yarn type/quality and thermoset matrix type on composite properties.

3.2 EXPERIMENTAL METHODOLOGY

3.2.1 Reinforcement materials

Four commercially available plant fibre yarns/rovings were used as composite reinforcements. The material properties of the four yarns are tabulated in Table 3.1, and have been determined by the author of this thesis (*Appendix A*). Notes on fibre/yarn processing are also provided in Table 3.1 Yarns have been named according to the fibre type (denoted by first initial) followed by the twist level in turns per meter (tpm); so, J190 is a jute yarn with a twist level of 190 tpm. The selected yarns enable studying the effect of fibre/yarn type (jute, hemp and flax) and fibre/yarn quality (F50 and F20) on PFRP mechanical performance. Note that fibre

Shah DU, Schubel PJ, Clifford MJ, Licence P. Mechanical property characterization of aligned plant yarn reinforced thermoset matrix composites manufactured via vacuum infusion. *Polymer-Plastics Technology and Engineering*, 2014, 53(3): p. 239-253.

DU Shah Page | 63

^{*} This chapter is based on the peer-reviewed journal article:

quality is defined 'qualitatively' by the source of the fibre/yarn and the mechanical properties of the resulting composite. Here, F20 is considered as a flax yarn with high-quality fibres, while F50 is a flax yarn with low-quality fibres.

On a side note, Table 3.1 also presents the commercial price of these yarns at the time of writing. Note that significant scales of economy are linked with bulk orders. Nonetheless, it is clear that only jute yarn (produced in developing nations such as Bangladesh) is able to compete against E-glass in terms of cost. Flax and hemp yarns/rovings (often produced in China but processed in Europe [2]), are up to 10 times more expensive than E-glass. Clearly, yarns of temperate fibres (flax and hemp) are not cost-viable substitutes to E-glass for composite reinforcement.

3.2.2 Production of unidirectional mats

For use as aligned reinforcements, the yarns were processed in the form of unidirectional mats. The mats were prepared using a drum-winding system (Fig. 3.1). The semi-continuous process involved automatic winding of yarns around a rotating (~60 rpm) and traversing (~0.5 mm/sec) aluminium drum (Ø315 mm, 400 mm long) with periodic manual adjustments of yarns to minimize inter-yarn spacing. Once the drum length was covered, the monolayer winding was uniformly hand painted with 0.6 wt% aqueous hydroxyethylcellulose (HEC) solution and dried at 60 °C for 30 min. HEC was purchased from Dow Chemical (Cellosize HEC OP-52000H). The mat was then recovered upon drying and cut to size (250×250 mm²). The HEC binding agent ensured that the mat held together. Although the binding agent application process is crude with little control over film thickness, the process effectively allowed the production of unidirectional mats with a high degree of alignment and controlled areal density (300-400 \pm 32 gsm). The binding agent accounted for 1-3 wt% of the mat. Importantly, the binding agent is cellulose-based (i.e. with surface properties similar to plant fibres) and thus has no significant effect on the properties of the resulting composite. This was confirmed (presented in Appendix B) through tensile tests on F50/polyester composites manufactured with i) mats produced using the technique outlined previously, and ii) stitched mats supplied by Formax (UK) Ltd.

Table 3.1. List of plant fibre materials and their properties.

Yarn ID	Fibre type	Fibre density † $ ho_f$ [gcm $^{-3}$]	Nominal linear density [tex]	True linear density [†] [tex]	Nominal twist level T [tpm]	Surface twist angle [†] α [°]	$egin{array}{c} ext{Yarn} \ ext{diameter}^\dagger \ ext{d_y} \ ext{[mm]} \end{array}$	Packing fraction [†] •	$Price^* \ C_f \ [\pounds/kg]$	Supplier	Notes on yarn processing ^Ψ
J190	Jute	1.433 ± 0.005	250	206 ± 21	190	20.5 ± 5.9	0.428	0.596	~1.1	Janata and Sadat Jute Ltd (Bangladesh)	Water retted fibres; Z-twist ring spun (dry) yarns; batching oil used as lubricant
H180	Hemp	1.531 ± 0.003	285	278 ± 17	180	19.5 ± 4.3	0.480	0.591	~7.6	Safilin (Poland)	Dew retted fibres; Relatively higher shive content; Z-twist ring spun (dry) yarns
F50	Flax	1.529 ± 0.003	250	229 ± 22	50	4.9 ± 3.8	0.437	0.421	~10.0	Composites Evolution (UK)	Dew retted fibres; Z-twist core flax yarn with S-twist polyester filament binder (13 wt%)
F20	Flax	1.574 ± 0.004	400	396 ± 16	20	0.5 ± 0.2	0.506	-	~13.3	Safilin (France)	Dew retted fibres; Z-twist ring spun (wet) rovings; fibres boiled in dilute NaOH prior to spinning

[†] Characterised and measured in *Appendix A*. Note that the measured fibre density is the absolute density (*i.e.* excluding the lumen) including moisture (typically 10 wt%). Also, the yarn diameter is based on a measured cross-sectional area (using pycnometry), and assuming circular cross-section. However, due to the low-twist and thus low packing fraction of F20, it is a roving with a non-circular cross-section.

^{*} The price of yarn/roving quoted is approximate and based on small quantities. Prices reduce significantly with high quantities (>5 tonnes). For reference, the price of raw flax/hemp fibre ranges between 0.5-1.5 £/kg, while the price of E-glass is $C_f \approx 1.3$ £/kg [1].

Ψ Further notes on fibre/yarn processing: During the fibre extraction process, the tropical jute fibres have undergone water retting (a more controlled but water-polluting process), while fibres from the temperate region (flax and hemp) have undergone dew/field retting (a strictly natural process influenced by actual weather conditions). Different batches of fibres were mixed, to ensure consistent yarn quality. All yarn batches consisted of several bobbins of yarn. None of the yarns were dyed or coated with wax to facilitate any subsequent dyeing process. Textile yarns J190 and H180 were obtained in high twist. For the former, 'jute batching oil' was used as a lubricant to increase yarn regularity during the drafting process. F50 is a low-twist flax with a polyester binder yarn, while F20 is a flax roving. F20 is the only yarn produced in a wet-spun process, where the fibres are soaked in a hot dilute solution of NaOH before spinning; this process improves defibration and yarn regularity.

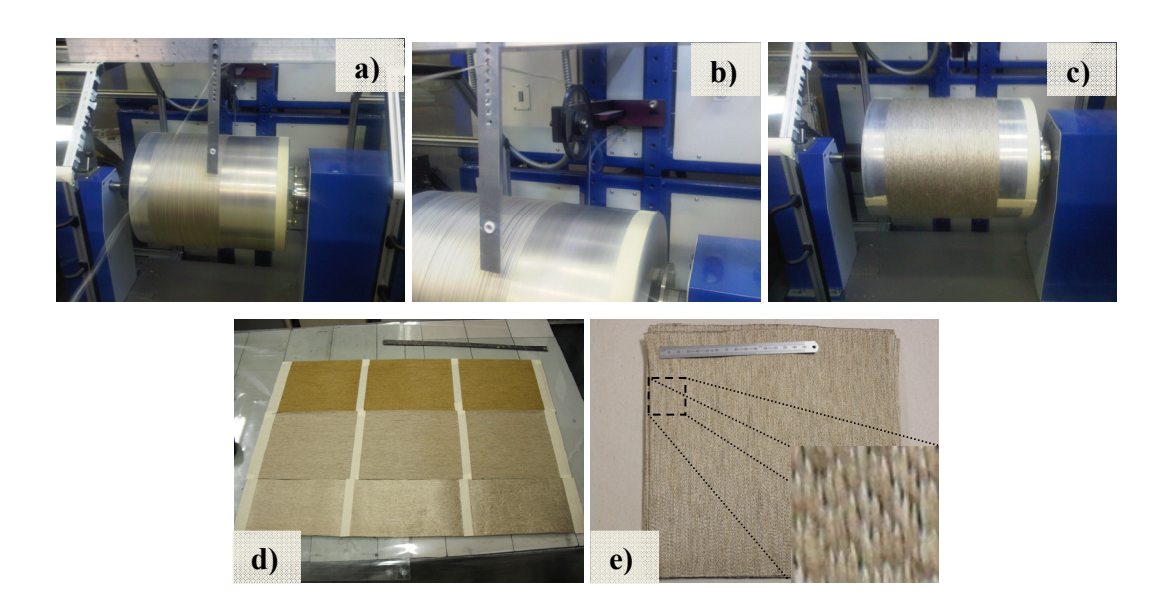


Fig. 3.1. Developed unidirectional mat fabrication process: a) Automatic winding of yarn around a drum; b) close-up of yarn guide and roller; c) manual shifting of yarn (if required) to produce a completed mono-layer winding; d) recovered mat after applying HEC binding agent and drying; e) single layer mat $(250 \times 250 \text{ mm}^2)$.

3.2.3 Manufacture of composites

Unidirectional PFRP laminates (250×250 mm², 3–3.5 mm thick) were fabricated using the vacuum infusion technique (Fig. 3.2). For each plaque, four layers of the reinforcement mat were used as-produced (without any preconditioning, such as drying). The mould tool includes a transparent Perspex top, a steel picture frame (~3 mm thick) and an aluminium base (Fig. 3.2a). Resin infusion was carried out at 70-80% vacuum (200-300 mbar absolute) at ambient temperature. The Perspex top had central and side resin injection/evacuation ports. Preliminary tests illustrated that due to the unidirectional fibre architecture, central injection produced non-isotropic ovular resin flow. On the other hand, line-gate injection perpendicular to the yarn axis generated uniform axial resin flow. Hence, the latter was the preferred method of resin injection (Fig. 3.2b).

Two standard thermoset resins were used as matrices for composite fabrication: *i)* unsaturated polyester (UP) type 420-100 (mixed with 0.25 wt% NL49P accelerator (1% Cobalt solution) and 1 wt% Butanox M50 MEKP initiator), and *ii)* low-viscosity

Epoxy Prime 20LV (mixed with its fast hardener at a 100:26 mass ratio). For both resin systems, post cure was carried out at 55 °C for 6 h after ambient curing for 16 h. Table 3.2 presents datasheet properties of the cured resin systems. Note the similarity in properties of the two thermosetting matrices. The matrix shear modulus G_m is estimated using Eq. 3.1, assuming a matrix Poisson's ratio v_m of 0.38 [3-5].

$$G_m = \frac{E_m}{2(1 + V_m)}$$
 Eq. 3.1

Using stitched unidirectional E-glass fabric (1200 ± 32 gsm) obtained from Formax (UK) Ltd, aligned GFRPs were similarly manufactured as reference materials.

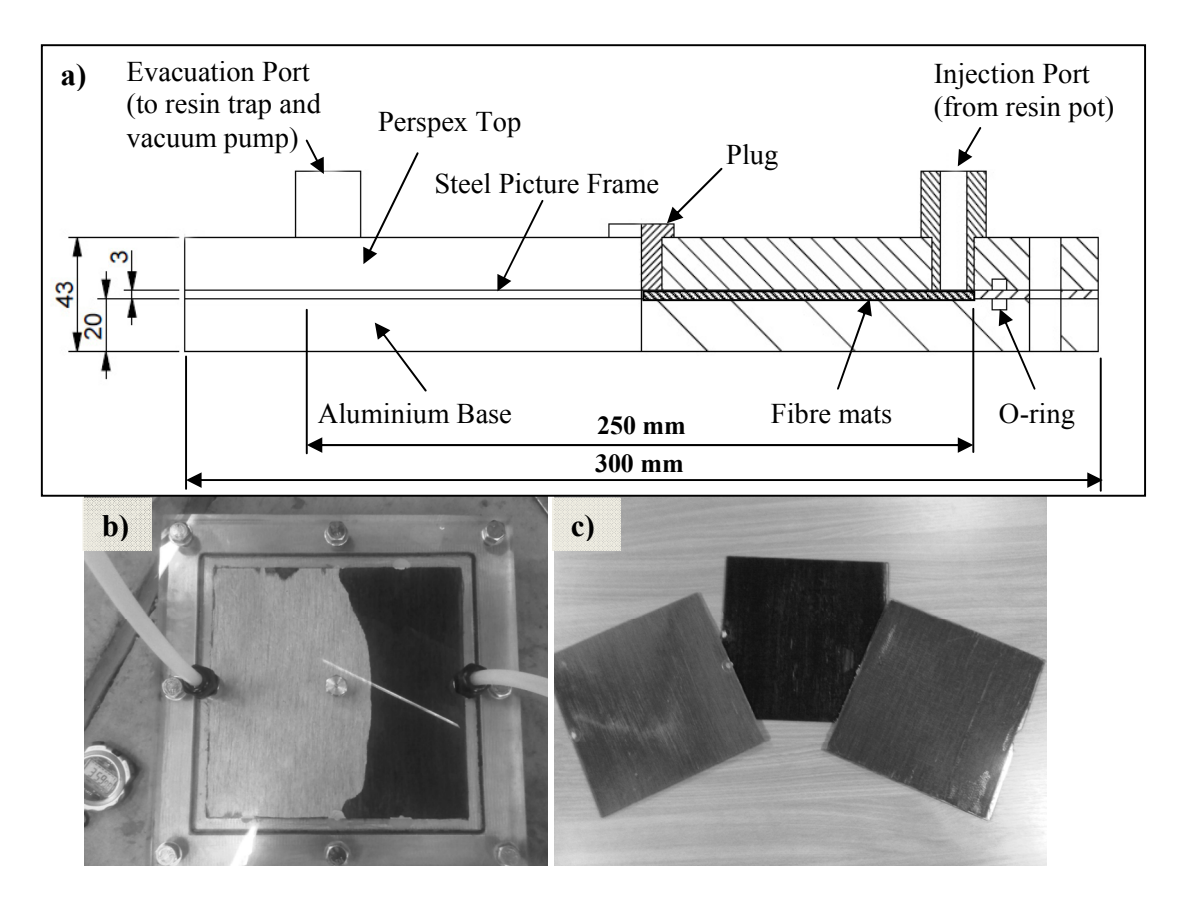


Fig. 3.2. Composite manufacturing process: *a)* schematic of the mould tool, images of *b)* the infusion process, and *c)* the produced composite laminates.

Table 3.2. Resin systems and their datasheet properties.

Resin	Supplier	Mixed viscosity [mPas] or [cP]	Geltime at 25 °C [mins]	Cured density ρ_m [gcm ⁻³]	Tensile modulus E_m [GPa]	Tensile strength σ_m [MPa]	Failure strain ε_m [%]	Shear modulus G_m [GPa]
UP	Reichhold Norpol	210	30	1.202	3.7	70	3.5	1.34
Epoxy	Gurit UK Ltd	230	30	1.153	3.2	75	4.1	1.16

3.2.4 Physical characterisation

The fibre weight fraction w_f of a laminate was calculated using the ratio of the mass of the preform W_f and the resulting laminate W_c . The fibre and matrix densities have been presented in Table 3.1 and Table 3.2. The composite density ρ_c was measured using a calibrated Micromeritics AccuPyc 1330 helium pycnometer. A purge fill pressure of 19.0 psig, equilibrium rate of 0.05 psig/min and specimen chamber temperature of 20 ± 1 °C was used. For each laminate a minimum of five samples were tested, where the final density reading for each sample was an average of five systematic readings (from five purges/runs). The fibre volume fraction v_f , matrix volume fraction v_m and void volume fraction v_p of the composites were then determined using equation Eq. 3.2, where w and ρ represent weight fraction and density, respectively while the subscripts f, m and c denote fibres, matrix and composite, respectively.

$$v_f = \frac{\rho_c}{\rho_f} w_f; \quad v_m = \frac{\rho_c}{\rho_m} (1 - w_f); \quad v_p = 1 - (v_f + v_m)$$
 Eq. 3.2

Optical microscopy was then used to qualitatively image the fibre/yarn packing arrangement and porosity in the composites. For this, three cross-sections from each composite were cast (using casting polyester resin), polished (using 100, 200, 300, 600, 800, 1200 and diamond grit paper) and viewed under a microscope. Images were processed using ImageJ software.

3.2.5 Testing of mechanical properties

For all studies in this thesis, all composite samples were stored for at least 48 hours at ambient conditions before any testing. The composite plaques were cut with a high-speed abrasive/diamond cutting machine, without any lubrication fluid (to avoid

moisture intake), to produce specimens for testing. All mechanical testing was conducted under ambient conditions (typically, 15-25 °C and 60-90% relative humidity).

3.2.5.1 Short-beam shear test

Short-beam shear tests were carried out according to ASTM D2344, where unnotched specimens were loaded in a three-point bending configuration at a cross-head speed of 1 mm/min. An Instron 5969 testing machine equipped with a 2 kN load cell was used for these tests. The width b and length l of the test specimen was kept at 2 and 6 times the thickness t, respectively. A span-to-thickness (L_0/t) ratio of 4:1 was used; the chosen L_0/t ratio encourages failure of specimen through interlaminar shear along the neutral axis, rather than inelastic deformation or flexural failure in compression/tension on the surface. The 'apparent' interlaminar shear strength τ was calculated using Eq. 3.3, where P is the maximum applied load. Six specimens were tested for each type of composite.

$$\tau = \frac{3}{4} \frac{P}{ht}$$
 Eq. 3.3

3.2.5.2 Tensile test

Longitudinal tensile tests were conducted according to ISO 527-4:1997 using an Instron 5985 testing machine equipped with a 100 kN load cell and a 50 mm extensometer. Six 250 mm long and 15 mm wide specimens were tested for each type of composite at a cross-head speed of 2 mm/min. 'Specimen Protect' was used to ensure that the specimens weren't damaged during gripping. The tensile modulus E_c (in the strain range of 0.025–0.100%), ultimate tensile strength σ_c , and tensile failure strain ε_c were measured from the stress-strain curve.

3.2.5.3 Impact test

The impact properties of the composites were determined using an Avery Denison pendulum Charpy testing machine according to ISO 179:1997. The un-notched specimens were loaded flat-wise with weighted hammers at a point perpendicular to the direction of the unidirectional fabric plane. A 2.7 J hammer was used for PFRPs

while a 15 J hammer was used for GFRPs. A striking velocity of 3.46 ms⁻¹ was used. Six specimens (100 mm long and 10 mm wide) were tested for each type of composite. The impact strength (or work of fracture) was determined by dividing the measured fracture energy with the specimen cross-sectional area.

3.3 RESULTS AND DISCUSSION

3.3.1 Manufacturing properties

3.3.1.1 Physical properties

Density and fibre volume fraction

Physical properties of the manufactured laminates are presented in Table 3.3. Matrix type has little effect on composite density as the matrices used in this study have very similar densities. As expected, due to the 40-50% lower density of plant fibres compared to E-glass, PFRPs are significantly lighter (30-40%) than GFRPs.

Table 3.3. Physical properties of manufactured laminates (mean \pm stdev).

		Fibre weight fraction	Composite density	Fibre volume fraction	Void volume fraction	Cost of composite panel [†]
Unidirectional reinforcement	Resin System	w_f [%]	$ ho_c$ [gcm ⁻³]	[%]	$egin{array}{c} oldsymbol{v_p} \ oldsymbol{[\%]} \end{array}$	$egin{array}{c} C_c \ [\mathbf{\pounds}] \end{array}$
E-glass	Epoxy	63.7	1.782 ± 0.009	42.6 ± 0.2	1.3 ± 0.5	1.62
J190	Epoxy	40.5	1.236 ± 0.006	34.9 ± 0.2	1.3 ± 0.5	1.47
H180	Epoxy	40.6	1.259 ± 0.009	33.4 ± 0.3	1.8 ± 0.7	2.22
F50	Epoxy	32.9	1.249 ± 0.002	26.9 ± 0.1	0.5 ± 0.2	2.45
F20	Epoxy	36.9	1.273 ± 0.004	29.9 ± 0.1	0.5 ± 0.3	2.26
E-glass	UP	63.6	1.793 ± 0.035	42.8 ± 0.8	2.9 ± 1.9	0.63
J190	UP	37.1	1.226 ± 0.010	31.7 ± 0.3	4.2 ± 0.8	0.46
H180	UP	41.9	1.303 ± 0.004	35.6 ± 0.2	1.3 ± 0.4	1.09
F50	UP	33.0	1.282 ± 0.004	27.7 ± 0.1	0.9 ± 0.3	1.25
F20	UP	37.3	1.304 ± 0.008	30.9 ± 0.2	1.0 ± 0.6	1.64

[†]The materials cost is estimated using $C_c = W_c(C_f w_f + C_m(1-w_f))$, where the cost of the matrix C_m is taken to be 2.50 and 10.00 £/kg for polyester and epoxy, respectively. Note that the cost is 'normalised' for composite volume, where the volume is approximately equal at $3\times250\times250 \text{ mm}^3$.

For the composites produced (Table 3.3), the fibre volume fraction of unidirectional GFRPs (~43%) is higher than that of PFRPs (27–36%). These findings are in agreement with other studies in literature. Producing composites by compression moulding, Madsen *et al.* [6] report that for a constant compaction pressure, unidirectional flax yarn and E-glass composites have a fibre volume fraction of 56% and 71%, while random flax fibre and E-glass composites have a fibre volume fraction of 38% and 52%, respectively. Goutianos *et al.* [7] also find that when employing liquid moulding processes (specifically, hand lay-up and RTM), GFRPs produce higher fibre volume fractions than PFRPs. In essence, random fibre composites produce lower fibre volume fractions than aligned fibre composites, and PFRPs produce lower fibre volume fractions than GFRPs.

Madsen *et al.* [6] argue that fibre alignment and degree of fibre separation affect the compact-ability of a preform. Synthetic fibre assemblies have higher packing-ability than plant fibre assemblies [6, 8]. This is because unidirectional synthetic fibre assemblies are made of rovings with continuous, parallel and uniform (diameter) fibres that are well-separated, while unidirectional plant fibre assemblies are made of yarns with discontinuous, twisted and non-uniform (diameter) fibres that are typically in bundles/clusters. This is confirmed through optical microscopy images (Fig. 3.3a and d).

Typically, the maximum attainable fibre volume fraction for unidirectional GFRPs is of the order of 70-80% [4]. The upper limit for unidirectional PFRPs is in the range of 50–60% [8]. This lower maximum attainable fibre volume fraction is a set-back for PFRPs as composite mechanical properties generally improve with fibre volume fraction.

It is important to note that the manufacturing technique also has a significant effect on achievable fibre volume fractions. For instance, compression moulding or hotpressing would produce higher fibre volume fractions than vacuum infusion and even RTM (as discussed in *Chapter 2*). This is because in compression moulding the compaction pressure and preform mass can be adjusted to achieve a pre-desired laminate thickness and fibre volume fraction. Commercially, PFRPs are primarily

produced via compression moulding [2]. However, this study employs vacuum infusion as it enables the cost-effective manufacture of large geometrically-intricate components, such as wind turbine blades, in low volumes. As an extension to this study, the possibilities of using vacuum-assisted RTM or prepregging for the manufacture of higher fibre content (and lower void content) PFRPs could be considered. For instance, Weyenberg *et al.* [9] and Baets *et al.* [10] have been able to produce flax/epoxy composites with $v_f \approx 50\%$ using prepreg technology.

Table 3.3 also presents the deviations in the measured readings of density and fibre volume fraction. The standard deviations for PFRPs are low (~1% of the mean values) and comparable to GFRPs, implying that they are producible with consistent and uniform fibre distribution. This is valuable if PFRPs are to be considered for structural applications.

Reinforcement packing

Fig. 3.3 shows micrographs of cross-sections in *a)* J190, *b)* H180, and *c)* F20 yarn PFRPs. While it is observed that on a macro-scale yarn bundles in high-twist yarn PFRPs (J190/H180) are distributed relatively uniformly within the matrix and the fibres in the yarn are well impregnated (Fig. 3.3a and b), on a meso-scale the fibre distribution is distinctly heterogeneous. That is, the distribution of fibres within the compact yarn is concentrated/clustered and there are noticeable resin-rich regions. On the other hand, in low twist-low compaction F20 yarn preforms (Fig. 3.3c), inter-yarn spaces are comparable to intra-yarn spaces. In fact, individual rovings are difficult to distinguish. Hence, fibre distribution is more uniform and the fibres are well-separated. This is similar to the distribution of fibres in unidirectional GFRPs (Fig. 3.3d). Such homogeneity in fibre distribution would allow better distribution of stresses/strains upon loading.

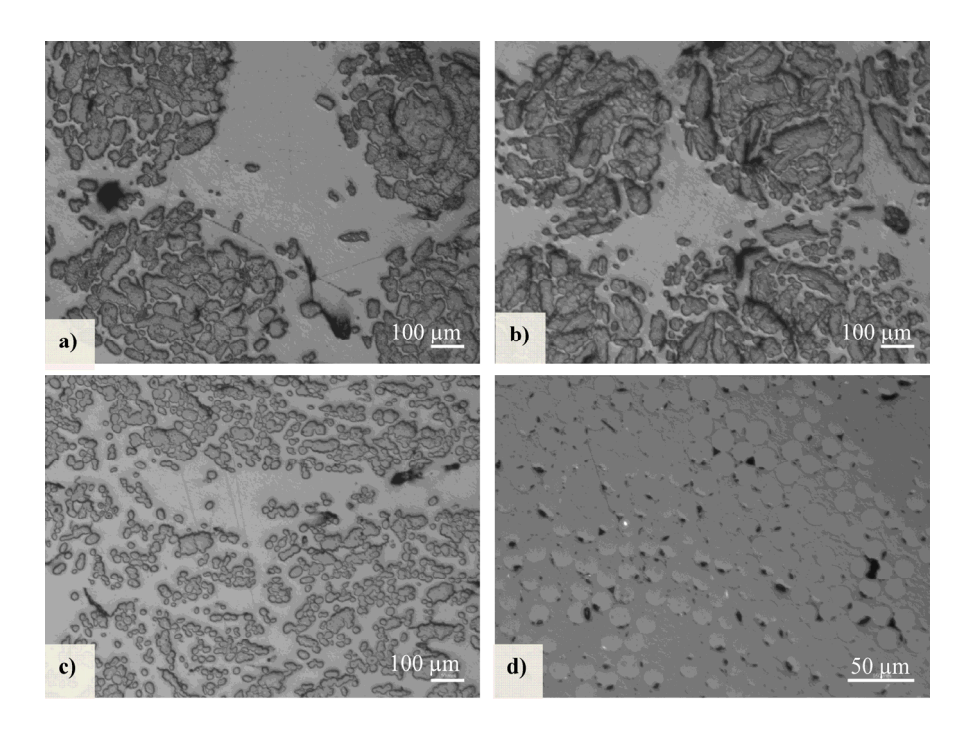


Fig. 3.3. Microscopy images of a) J190 and b) H180 epoxy composites showing the large difference in inter-yarn and intra-yarn spacing and inhomogeneous fibre distribution compared to c) F20 and d) E-glass epoxy composites. Also notice the constant diameter of E-glass, but non-uniform cross-sectional shape and width of plant fibres.

Porosity

The void content of aligned PFRPs is found to be in the range of 0.5-2%, with the exception of J190/polyester, which has a higher void content of 4.2%. Nonetheless, the void content of PFRPs is comparable to that of GFRPs (1-3%). Typically, void contents of <1% are required for aerospace applications, but void contents of up to 5% are acceptable for other less demanding applications (*e.g.* automotive and marine) [11-13].

In literature [8, 14, 15], PFRPs are often quoted to have high void content. Typically, the void volume fraction is up to 5% for PFRPs with a fibre volume fraction below 40% [8, 16-20]. However, when the fibre volume fraction exceeds 40%, void content increases drastically and can even approach 20% [8, 17-19, 21]. Nonetheless, there are some studies [16, 22] which conclude that there is no obvious relationship between PFRP fibre volume fraction and void volume fraction. From the literature

survey, it is suggested that issues of high porosity in PFRPs are usually related, but not confined, to i) sisal fibre composites due to the large lumen size in sisal fibres which remain unfilled after resin infusion [20, 21], ii) structural porosity in (particularly, high weight fraction) compression-moulded thermoplastic PFRPs due to insufficient amount of matrix to fill the free space between the yarns [8], and iii) randomly-oriented short-fibre PFRPs. In this work, comparatively lower void contents have been observed which is in agreement with other studies that use thermoset resins in a vacuum infusion process [20]. Perhaps, the low viscosity of thermoset resins (Table 3.2) allows better impregnation of plant fibre assemblies. In fact, Madsen $et\ al.$ [6] show that porosity in hemp yarn reinforced thermoplastics increases linearly ($R^2 = 0.98$) with the logarithm of the matrix processing viscosity. As the viscosity of thermosets is several orders of magnitude lower than that of thermoplastics, the lower void content in thermoset-based PFRPs is understandable.

This study uses yarns as a form of continuous reinforcement with controlled orientation. It is has been suggested that the twisted nature of such yarns leads to a tightened/compact structure (as observed in Fig. 3.3a), which may cause reduced permeability, hindered impregnation, and thus void formation [16, 23]. Consequently, increasing yarn twist is likely to worsen these issues. However, in their experimental study, Zhang *et al.* [16] found no correlation between composite porosity and yarn structure. Even at different fibre volume fractions, the porosity content in PFRPs composing ring-spun yarns (surface twist angle of 30°) and commingled natural fibre/polypropylene yarns (surface twist angle of 0°) was similar and in the range of 1.4 to 5.2%. Indeed, in this study, the void content of yarn reinforced PFRPs is found to be low as well (0.5-4.2%).

While there may not be an obvious relationship between yarn structure and void content, the yarn structure may dictate the type of voids that form, particularly due to its effects on reinforcement packing and resin-flow dynamics. Madsen *et al.* [8] have described three categories of porosity in PFRPs: *i)* fibre-related porosity, *ii)* matrix-related porosity (characteristic of liquid moulding processes), and *iii)* structural porosity (characteristic of thermoplastic moulding processes). Fibre-related porosity can be broken down into further sub-components: *a)* luminal porosity (in the fibre

lumen), b) interface porosity (at the fibre/matrix interface) and c) impregnation porosity (between fibre bundles).

In this study, qualitative analysis suggests that fibre porosity related to unfilled luminal cavities in fibres make a larger contribution to the total porosity in jute composites, compared to hemp and flax composites (Fig. 3.4). This observation is in agreement with the literature [1, 8]. Noting that the typical diameter of jute fibres is almost double that of flax/hemp [1, 24, 25], the size of the luminal cavity in flax/hemp and jute fibres is typically 2-11% [1, 6, 8, 26] and 10-14% [1, 8, 27] of their cross-sectional area. However, it is arguable that luminal porosities may not be detrimental to the performance of PFRPs as they do not encourage stress concentration or fibre debonding [8]. In contrast, Baley *et al.* [28] find that the lumen encourages crack initiation, when a unidirectional PFRP is loaded in the transverse direction.

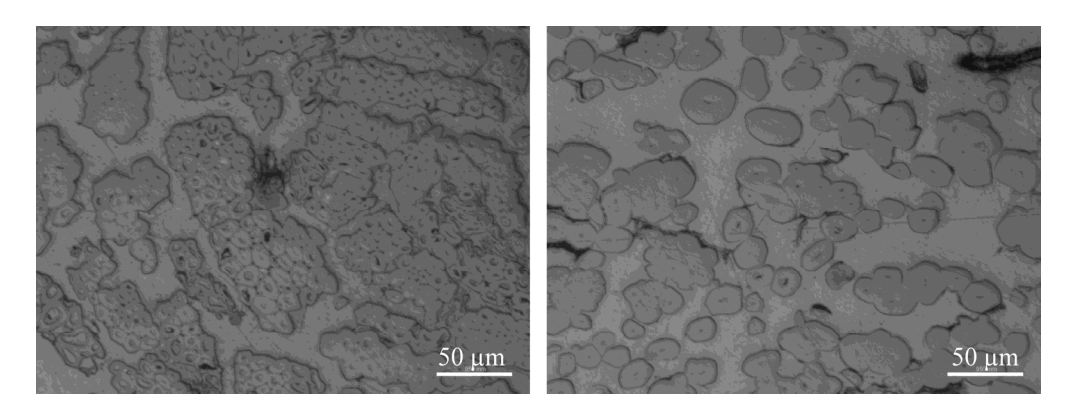


Fig. 3.4. Luminal spaces in fibres of jute (left) are larger than that in flax (right).

Microscopy of composite cross-sections also shows that porosity in high-twist yarn J190/H180 composites is primarily associated with impregnation porosity (Fig. 3.5a). Impregnation porosity is due to inadequate or poor matrix impregnation of the yarns [8] and in this case may be a result of high compaction of fibres and low permeability within the yarn. On the other hand, low-twist yarn F50/F20 composites are not susceptible to impregnation porosity due to the low compaction of fibre within the yarn/roving and thus a yarn permeability that is comparable to the preform permeability. Rather, low-twist yarn composites are primarily affected by interface

porosity (Fig. 3.5b). Although this is suggestive of poorer fibre/matrix compatibility in low-twist yarn PFRPs, this is not true because both low- and high-twist yarn PFRPs compose of hydrophilic plant fibres and hydrophobic matrices. A possible explanation is that high-twist yarns, particularly jute, are observed to consist of large fibre sub-assemblies (fibre bundles) within yarns (Fig. 3.3 and Fig. 3.5) while low-twist yarns, particularly flax, are more defibrillated into single fibres due to low compaction (Fig. 3.3 and Fig. 3.5). This means that in low-twist yarn PFRPs, the matrix needs to wet-out a relatively larger surface area of small fibre bundles (if not single fibres) as compared to smaller surface area of large fibre bundles.

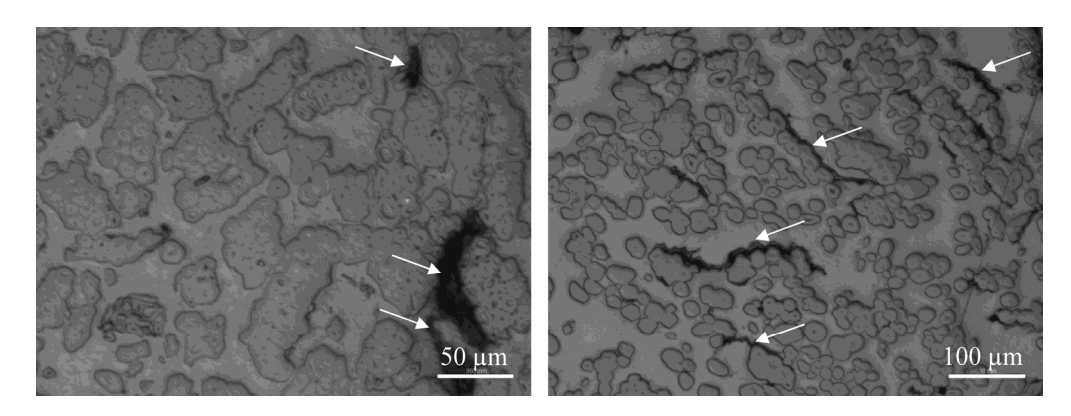


Fig. 3.5. Microscopy images of J190 (left) and F20 (right) epoxy composites. High-twist yarn J190 composites have impregnation-related porosities while low twist yarn F20 composites have interface-related porosities (indicated by arrows). High-twist yarns (particularly jute) consist of large fibre bundles, while fibres in low-twist yarns (particularly flax) are well-separated.

3.3.1.2 Materials cost

Table 3.3 presents the materials cost for each type of composite. It is clearly observed that *i*) epoxy composites are more expensive than polyester composites due to the significantly higher cost of epoxy matrix, and *ii*) PFRPs are more expensive than GFRPs. While raw plant fibres are cost-competitive to E-glass, plant fibre yarns/rovings (particularly from temperate fibres) are not cost-viable substitutes to E-glass for composite reinforcement. As cost is often a critical design criterion for industrial applications, employing such yarns for commercial PFRP applications is not foreseeable in the short-term future, unless plant yarn reinforcements become significantly cheaper.

3.3.2 Mechanical properties

3.3.2.1 Apparent interlaminar shear strength

Results from short-beam shear tests are presented in Fig. 3.6. Note that the determined results are not absolute values, but purely for relative comparison. The 'apparent' interlaminar shear strength τ is a measure of the strength of the matrix plus the interface. From Fig. 3.6, it is observed that epoxy composites display higher interlaminar shear strength compared to polyester composites. This is possibly because epoxy has a marginally higher estimated matrix shear strength (using Tresca criteria, $\tau_m = \sigma_m/2$) than polyester. In addition, the better adhesive properties of epoxy may make it more compatible with hydrophilic plant fibres and thus provide a stronger interface. This is in agreement with the results from impact tests and tensile tests (discussed in later sections).

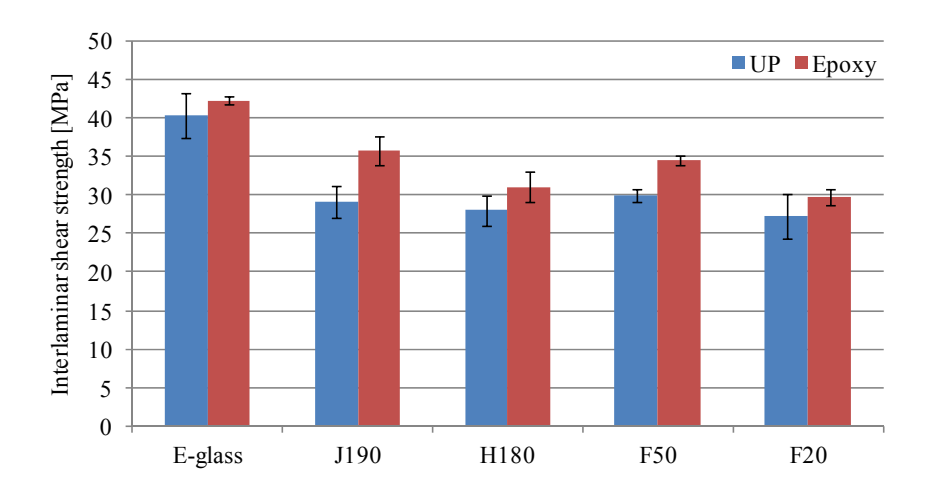


Fig. 3.6. Interlaminar shear strength of composites. Error bars denote 1 standard deviation.

It is observed that aligned GFRPs have 20-30% higher interlaminar shear strengths (40-42 MPa) than aligned PFRPs (ranging from 27-36 MPa). The study by Goutianos *et al.* [7] is in agreement with this finding. The higher interlaminar shear strength of GFRPs is a sign of better fibre/matrix adhesion. This is expected as *i*) synthetic fibres are often surface-treated after manufacture in order to improve the interfacial bond, *ii*) plant fibres are highly polar and form a weak interface with typically non-polar

matrices, and *iii*) unlike plant fibres whose surface energy is similar to that of the matrix, the surface energy of E-glass is significantly higher than that of the matrix facilitating good wet-out.

Amongst PFRPs, high-twist J190 yarn composites exhibit best interfacial properties while low-twist F20 composites display lowest properties. This is possibly due to the high content of interface-related porosities in F20 composites (as discussed in Section 3.3.1.1.3). It is also possible that the yarn construction (specifically, twist level) affects the composite interlaminar shear strength. Naik *et al.* [29] show that twisted resin-impregnated yarns show higher shear strength than straight impregnated yarns due to higher transverse pressure in twisted yarns. However, more investigations are necessary to elucidate the differences in the governing mechanisms of (shear) stress development in a single impregnated yarn compared to a yarn reinforced laminate.

Critical fibre length

The critical fibre length l_c and fibre aspect ratio l_f/d_f are important parameters that dictate mechanical properties of a composite. In particular, they define the fibre length efficiency factor; that is, the ability of the fibre to transfer strength and stiffness to the composite. Sub-critical length fibres ($l_f < l_c$) will not carry the maximum possible load. To efficiently utilise the fibre properties, either the critical fibre length l_c should be decreased below the fibre length l_f (by improving interfacial properties), or the reinforcing fibre length l_f (and thus aspect ratio) should be increased much above the critical fibre length l_c .

The critical fibre length l_c is defined by Eq. 3.4, where σ_f is the fibre tensile strength (at the critical fibre length), d_f is the fibre diameter, and τ is the interfacial strength. The estimated critical fibre length l_c for all the composites produced in this study is presented in Table 3.4. As inputs in Eq. 3.4, typical fibre strength σ_f and diameter d_f have been used from various sources.

$$l_c = \frac{\sigma_f d_f}{2\tau}$$
 Eq. 3.4

Table 3.4. Estimating the critical fibre length and fibre length efficiency factors for composite stiffness and strength.

Unidirectional reinforcement	Resin System	$Fibre$ $stiffness$ E_f $[MPa]$	Fibre strength o _f [MPa]	Fibre diameter d _f [µm]	Gauge length l [mm]	Source of single fibre properties	Typical fibre aspect $ratio^{\dagger}$	Critical fibre length l_c [mm]	Length efficiency for stiffness η_{IE}	Length efficiency for strength η_{IS}
E-glass	Epoxy	78.5	1956	13.8	50	[30]	>3000	0.320	0.999	0.996
J190	Epoxy	32.5	558	53.9	6	[25]	100	0.421	0.976	0.961
H180	Epoxy	24.7	636	27.6	8	[31]	900	0.283	0.998	0.994
F50	Epoxy	56.0	1099	17.5	10	[32]	1750	0.278	0.998	0.995
F20	Epoxy	56.0	1099	17.5	10	[32]	1750	0.323	0.998	0.995
E-glass	UP	78.5	1956	13.8	50	[30]	>3000	0.335	0.999	0.996
J190	UP	32.5	558	53.9	6	[25]	100	0.515	0.977	0.952
H180	UP	24.7	636	27.6	8	[31]	900	0.314	0.998	0.994
F50	UP	56.0	1099	17.5	10	[32]	1750	0.321	0.998	0.995
F20	UP	56.0	1099	17.5	10	[32]	1750	0.352	0.998	0.994

[†] Typical fibre aspect ratios are from [1, 6].

The critical fibre length l_c for epoxy composites is lower than that for polyester composites. Furthermore, the critical fibre length l_c for PFRPs is found to be in the range of 0.28-0.52 mm, which is comparable to that of GFRPs (0.32-0.34 mm). The estimated l_c for GFRPs is in agreement with values typically quoted in literature [4]. While there are some studies that determine l_c for PFRPs to be >2 mm [33-36], other studies report a smaller critical length l_c , similar to values found in this study, of 0.4-0.9 mm [33, 35, 37-39].

While plant fibres are naturally discontinuous, fibres employed in the production of yarns/rovings have lengths >25 mm [35, 40, 41]. Hence, in this study, the plant fibre reinforcements have high aspect ratios and are much longer than the critical length.

Fibre length efficiency factor

It is common for scientists working on plant fibre composites to assume that length efficiency factors are unity, when back-calculating fibre properties or predicting composites properties (for instance, [9, 10, 17, 21, 42]). However, it is important to assess if this claim is valid. The calculated critical fibre lengths l_c and typical values of fibre aspect ratio (length/diameter) l_f/d_f can be used to determine the length efficiency of the reinforcements. Cox's shear lag model [43] can be used for the calculation of the fibre length efficiency factor for stiffness η_{IE} , assuming iso-strain conditions, axial loading of fibres and elastic stress transfer between fibre and matrix. η_{IE} is given by Eq. 3.5, where G_m is the shear stiffness of the matrix, E_f is the stiffness of the fibre, and $v_{f,max,FRP}$ is the maximum achievable fibre volume fraction. Assuming square packing arrangement of continuous and parallel fibres, $v_{f,max,FRP}$ of $\pi/4$ (=78.5%) can be used. For the calculation of the fibre length efficiency factor for strength η_{IS} , Kelly-Tyson's model [44] can be used (Eq. 3.6), with $l_f > l_c$.

$$\eta_{IE} = 1 - \frac{\tanh\left(\frac{\beta l_f}{2}\right)}{\frac{\beta l_f}{2}}, \frac{\beta l_f}{2} = \frac{l_f}{d_f} \sqrt{\frac{2G_m}{E_f \ln\left(\sqrt{v_{f,\text{max},FRP}/v_f}}\right)}$$
 Eq. 3.5

$$\eta_{lS} = \begin{cases}
1 - l_c / 2l_f & for l_f \ge l_c \\
l_f / 2l_c & for l_f \le l_c
\end{cases}$$
Eq. 3.6

The calculated fibre length efficiency factors for stiffness and strength are found to be very close to unity for all the composites (Table 3.4). This is expected as high aspect ratio fibres ($l_f/d_f > 100$) are being used and the critical fibre length is very small ($l_f/l_c > 50000$). Madsen *et al.* [14] show that fibre aspect ratios of $l_f/d_f > 50$ would yield $\eta_{IE} > 0.93$ for plant fibre composites, and further increase in aspect ratio would asymptotically increase η_{IE} towards unity. Sawpan *et al.* [38] also determine η_{IS} to be 0.96 for their short-fibre ($l \approx 2$ -3 mm) hemp/polyester composites. These results confirm that like E-glass, plant fibres, particularly in the form of yarns, can deliver high length efficiency factors and thus, good load-transferring capabilities. Therefore, $\eta_{IE} = \eta_{IS} = 1$ is used for analysis in this thesis.

3.3.2.2 Tensile properties

The measured tensile properties of the composites are presented in Table 3.5. It is encouraging to note that although mechanical properties of single plant fibres are known to have high variability, at a composite scale, the tensile properties of PFRPs are consistent and with a small coefficient of variation of up to 6%, which is similar to that of GFRPs.

From the composite properties, the tensile stiffness E_f and strength σ_f of the reinforcing fibres has been 'back-calculated' using the rule of mixtures (Eq. 3.7, Eq. 3.8). The back-calculated fibre properties are useful in evaluating the reinforcing potential of plant fibres and comparing the tensile performance of the various composites at the same fibre volume fraction ($v_f = 100\%$). In light of the results from Section 3.3.2.1, the fibre length efficiency factors (η_{IE} and η_{IS}) have been taken to be unity. As in other studies [9, 10, 17, 42], the fibre orientation efficiency factor η_o is assumed to be unity for yarn reinforced unidirectional PFRPs and unidirectional GFRPs. In Eq. 3.8, σ'_m is the matrix stress at fibre failure strain ε_f . Assuming isostrain conditions, the fibre failure strain ε_f is equal to the composite failure strain ε_c . σ'_m is then estimated using Hooke's law to be $\sigma'_m = E_m \varepsilon_c$ [9].

$$E_f = \frac{E_c - v_m E_m}{\eta_{lE} \eta_o v_f}$$
 Eq. 3.7

$$\sigma_f = \frac{\sigma_c - v_m \sigma'_m}{\eta_{IS} \eta_o v_f}$$
 Eq. 3.8

Table 3.5. Tensile properties of manufactured composite laminates (measured; mean \pm stdev) and fibres (back-calculated; mean).

Unidirectional reinforcement	Resin System	Fibre volume fraction v _f [%]	Composite tensile modulus E_c [GPa]	Fibre tensile modulus E_f [GPa]	Composite tensile strength σ_c [MPa]	Fibre tensile strength σ_f [MPa]	Composite failure strain ε_c [%]
E-glass	Epoxy	42.6 ± 0.2	34.0 ± 2.1	75.6	705.7 ± 34.0	1603.7	1.3 ± 0.4
J190	Ероху	34.9 ± 0.2	15.0 ± 1.4	37.0	185.8 ± 16.2	441.1	1.6 ± 0.0
H180	Ероху	33.4 ± 0.3	19.0 ± 1.1	50.7	195.1 ± 8.9	477.3	1.7 ± 0.1
F50	Ероху	26.9 ± 0.1	14.2 ± 0.3	44.3	163.5 ± 3.0	449.6	1.8 ± 0.1
F20	Epoxy	29.9 ± 0.1	24.6 ± 0.4	75.1	281.4 ± 3.8	809.6	1.8 ± 0.1
E-glass	UP	42.8 ± 0.8	36.9 ± 1.4	81.6	825.7 ± 49.1	1843.0	1.9 ± 0.9
J190	UP	31.7 ± 0.3	16.1 ± 0.8	43.4	175.1 ± 10.3	442.4	1.5 ± 0.2
H180	UP	35.6 ± 0.2	17.0 ± 0.5	41.2	171.3 ± 6.5	368.8	1.7 ± 0.1
F50	UP	27.7 ± 0.1	15.6 ± 0.9	47.0	143.0 ± 6.8	368.2	1.6 ± 0.0
F20	UP	30.9 ± 0.2	23.4 ± 0.3	67.6	277.4 ± 8.2	760.5	1.7 ± 0.3

Effect of matrix type

There is some disagreement on the effect of matrix type on PFRP tensile performance in literature. Joffe *et al.* [45] find that while the difference in tensile properties of thermoset matrices (polyester, epoxy and vinylester) is large, the resulting randomly-oriented short-fibre flax composites have fairly indistinguishable tensile properties. They suggest that the fibre/matrix interface, and thus load transfer mechanisms and reinforcement efficiency, differ for different fibre/matrix combinations. On the other hand, Madsen *et al.* [17] observe that the noticeable difference in tensile properties of unidirectional hemp yarn reinforced thermoplastics can be correlated to the matrix type (PE, PP, PET). Madsen *et al.* [17] also report that the potential difference in fibre/matrix bonding, due to employing a different matrix, does not result in a visible effect on composite tensile properties or back-calculated fibre properties. Part of the discrepancy can be explained by the fact that compared to random composites, the fibres in unidirectional composites bear a much larger

fraction of the load, and hence interfacial properties would have little effect on longitudinal tensile properties [4].

In this study, there is no clear dependence of composite tensile performance on matrix type (Table 3.5), particularly due to the similar tensile properties of the thermoset matrices (Table 3.2). Comparing the back-calculated fibre tensile properties, it is observed that while E-glass and J190 reinforcements perform up to 15% better in a polyester matrix, H180, F50 and F20 reinforcements perform up to 20% better in an epoxy matrix. This implies that the reinforcing efficiency of the fibres and perhaps the fibre/matrix interfaces differ for the different matrices. It has been previously shown (Fig. 3.6) that all epoxy composites have higher 'apparent' interlaminar shear strength and thus presumably better fibre/matrix adhesion, compared to polyester composites. Hence, epoxy composites should display better longitudinal tensile properties. This, however, is not observed in the presented tensile test results.

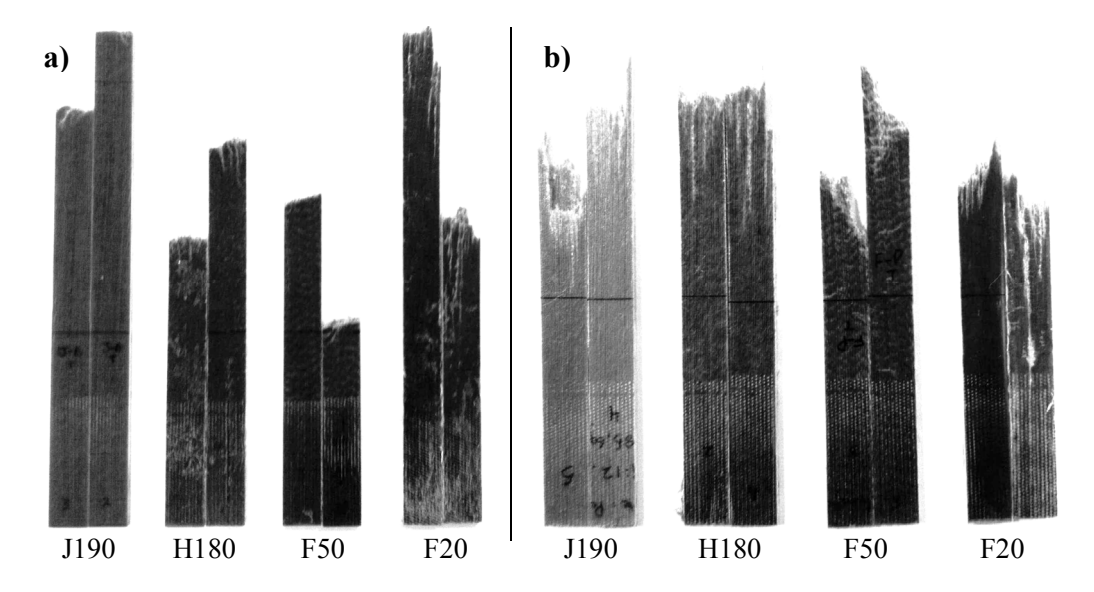


Fig. 3.7. Tensile fracture surface of a) epoxy- and b) polyester-based PFRPs.

Notably, the failure characteristics are different for epoxy- and polyester-based PFRPs (Fig. 3.7), which possibly relate to the difference in fibre/matrix interface properties [6]. It has been previously shown that the 'apparent' interlaminar shear strength of epoxy composites is better than that of polyester composites. Tensile

fracture specimens of epoxy composites display a fairly flat brittle fracture surface with little fibre pull-out resulting from matrix crack growth transverse to the fibre direction. On the other hand, fracture specimens of polyester composites display a more serrated failure surface with extensive fibre pull-out, and even delamination and longitudinal splitting, resulting from shear-induced micro-crack growth along the weaker fibre/matrix interface (that is, along the fibre axis) followed by macro-crack propagation through the micro-voids.

Effect of reinforcement type

Comparison of PFRPs with GFRPs

Comparing the effect of reinforcement type on tensile properties (keeping in mind the differences in fibre volume fractions), it is found that unidirectional GFRPs outperform unidirectional PFRPs in terms of tensile strength and stiffness (Table 3.5). E-glass composites are observed to have a tensile strength and stiffness of about 700-825 MPa and 34-37 GPa, respectively. This is considerably higher than the tensile strength and stiffness of PFRPs, which ranges between 140-285 MPa and 14-25 GPa, respectively. Notably, PFRPs and GFRPs have a similar tensile failure strain. It is worth pointing out that the better mechanical properties of unidirectional GFRPs (in comparison to unidirectional PFRPs) is not only due to the superior mechanical properties of the reinforcing E-glass fibres (in comparison to plant fibres), but also due to critical structural differences in the reinforcements. While aligned GFRPs employ continuous fibres that are almost perfectly aligned/parallel, aligned PFRPs employ yarns/rovings that have discontinuous fibres that are twisted.

An advantage of plant fibres over E-glass fibres for reinforcements is their 40-50% lower density. Hence, the specific properties of the composites are of interest; particularly as specific tensile modulus E_c/ρ_c and strength σ_c/ρ_c are often used as material selection criteria for components loaded in pure tension [46]. Fig. 3.8 plots the specific tensile properties of epoxy-based PFRPs relative to E-glass/epoxy composites. It is clearly observed that the density of PFRPs is about 40% lower than that of GFRPs. In addition, the specific tensile modulus E_c/ρ_c of J190, H180 and F50 composites is 60-80% that of unidirectional GFRPs, whereas F20 composites have a

specific tensile modulus that is similar to unidirectional GFRPs. Similarly, while the specific tensile strength σ_c/ρ_c of J190, H180 and F50 composites is ~40% that of unidirectional GFRPs, F20 composites have a specific tensile strength that is ~60% that of unidirectional GFRPs. Note that increasing the fibre volume fractions of the PFRPs would improve the specific tensile performance of PFRPs further. Nonetheless, the findings suggest that while high-quality unidirectional PFRPs may offer comparable specific stiffness performance to unidirectional GFRPs, the specific strength performance of PFRPs is poor.

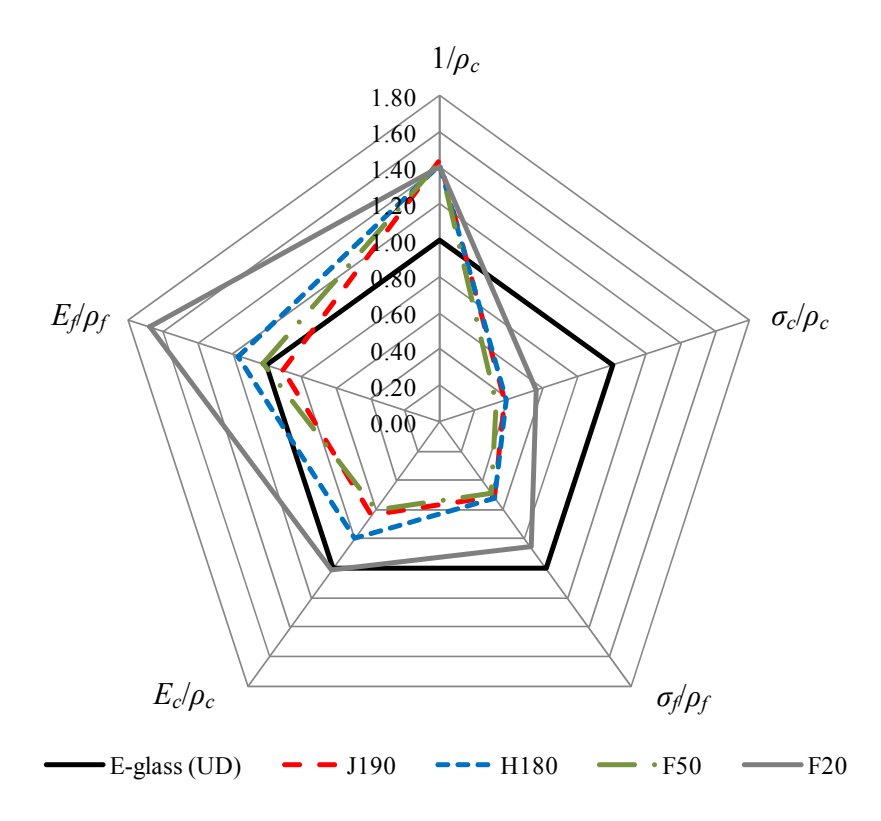


Fig. 3.8. Specific tensile properties of epoxy composites (measured) and fibres (back-calculated) relative to E-glass composite properties.

Back-calculated fibre properties have also been determined (Table 3.5). E-glass is estimated to have a tensile stiffness and strength in the range of 76-82 GPa and 1600-1850 MPa, respectively. This in agreement with typically reported literature values [1, 4, 30]. The results show that J190, H180 and F50 reinforcements have a tensile stiffness and strength in the range of 35-50 GPa and 360-480 MPa, respectively. This

is much lower than that of E-glass, but in the range of typically reported literature values [1]. Impressively, F20 flax reinforcements have a tensile stiffness which is comparable to that of E-glass at 67-75 MPa, and a tensile strength half that of E-glass at about 800 MPa. This is indeed a revelation and proof that flax has the reinforcing potential to replace E-glass in stiffness-critical structural applications.

Using the back-calculated fibre properties, specific tensile properties of plant fibres, relative to E-glass, are presented in Fig. 3.8. It is clearly observed that the specific stiffness performance of single plant fibres E_f/ρ_f is comparable to or even significantly outperforms that of E-glass, while the specific strength of plant fibres can range from 50-90% of E-glass. These findings confirm that at the same fibre volume fraction, plant fibres can provide a light and stiff alternative to E-glass reinforcements.

Effect of plant yarn reinforcement

All PFRPs have very similar tensile failure strain. In terms of tensile stiffness and strength, F20 composites clearly outperform the other PFRPs (Table 3.5). Comparatively, J190 and H180 composites have similar tensile properties, while F50 composites have the poorest tensile properties. While F20 composites have a tensile stiffness and strength of 23-25 GPa and 275-285 MPa, the other PFRPs have lower tensile stiffness and strength of 14-19 GPa and 140-200 MPa, respectively.

The dissimilarity in mechanical properties of the PFRPs may be a result of several factors. Firstly, the plant fibre type will affect the composite properties. Although plant fibre properties are subject to significant natural variation, typically, flax fibres have better mechanical properties than jute and hemp fibres (Table 3.6). As jute and hemp have better or similar cellulose content, cellulose crystallinity, degree of polymerisation (DP) and microfibril angle (MFA) in comparison to flax (Table 3.6), perhaps the significantly higher fibre aspect ratio of flax results in a higher fibre tensile strength. McLaughlin *et al.* [47] and Mukherjee *et al.* [48] have demonstrated the strong correlation between the structure (cellulose content, MFA and aspect ratio) and tensile properties (strength, modulus and failure strain) of plant fibres. Secondly, fibre/yarn quality will have an inevitable effect on composite properties. For instance,

although both F20 and F50 composites have similar volumetric composition and are made from low-twist flax rovings/yarns, there is a 40% difference in their tensile strength. Madsen *et al.* [49, 50] and Baets *et al.* [10] have shown that an increasing number of defects and an increasing number of processing steps can reduce fibre/yarn quality and thus composite properties. Thirdly, reinforcement construction will have an effect on the properties of the resulting composite. For instance, the hampered performance of F50 composites may be due to the inclusion of polyester as a filament binder in F50 yarn. It is also suggested that increasing yarn twist reduces composite mechanical properties like an off-axis laminate [23]. (This is studied in more detail in *Chapter 5*.) The F20 flax rovings have a significantly lower twist level than J190/H180 yarns, and thus F20 composites would bear minimal effects of reinforcement misorientation. As the yarn construction of J190 and H180 is similar (Table 3.1), and the mechanical properties of jute and hemp fibres are similar (Table 3.6), the comparable mechanical properties of J190 and H180 composites are likely.

Table 3.6. Structural and mechanical properties of bast fibres [1, 6, 51].

Fibre type	Cellulose content [%]	Cellulose crystallinity [%]	DP*	MFA [†] [°]	Aspect ratio	Tensile modulus [GPa]	Tensile strength [MPa]	Failure strain [%]
Flax	64–71	50-70	2420	5-10	1750	30-70	400-1100	2.7-3.2
Hemp	70–74	50-70	2300	2–6	900	30-60	300-800	1.3 - 2.7
Jute	61–72	50-70	1920	8	100	20-55	200-600	1.4-3.1

^{*}DP = degree of polymerization

The estimated fibre properties (Table 3.5) are found to be in the range of literature values (Table 3.6). While fibres from J190, H180 and F50 yarns have a tensile stiffness and strength in the range of 35-50 GPa and 360-480 MPa, respectively, F20 reinforcements have a tensile stiffness of 65-75 MPa and a tensile strength of about 800 MPa. It is noteworthy that such high mechanical properties of the plant fibres, particularly F20 flax fibres, have been transferred to the composites without any active fibre surface treatment.

[†]MFA = microfibril angle

A literature survey of tensile properties of unidirectional bast fibre reinforced composites is presented in Table 3.7. The measured tensile properties of aligned PFRPs obtained in this study are generally comparable with the results reported in literature. However, some flax composites are observed to have much higher tensile properties than those observed in this study. For instance, Baets *et al.* [10] report a tensile strength and stiffness of 378 MPa and 39.9 GPa for unidirectional flax/epoxy composites ($v_f = 42\%$). They employed minimally-processed (*i.e.* low defect count) hackled flax. Oksman *et al.* [52] also produce flax/epoxy composites ($v_f = 42\%$) with high strength and stiffness of 280 MPa and 35 GPa. They used flax fibres that were extracted in a biotechnical retting process using enzymes and microbial cultures. The extraction process is more environmentally friendly than traditional retting processes and produces fibres that are of uniform quality and more suitable for composites applications. Both studies employed slivers, as a more aligned reinforcement than a roving or a yarn, at high fibre content. In addition, no fibre surface modification techniques, to enhance interfacial properties, were employed in either study.

The back-calculated fibre properties presented in literature (Table 3.7) are also comparable to those obtained in this study (Table 3.5). It is of interest to note that while jute and hemp reinforcements have a tensile stiffness in the range of 30-55 GPa, flax reinforcements consistently deliver higher stiffness; usually in excess of 60 GPa, and up to 90 GPa. Furthermore, flax fibres offer higher reinforcement strength in the composite. Indeed, in this study, F20 flax reinforcements have an impressive back-calculated fibre stiffness and strength of up to 75 GPa and 800 MPa, respectively.

Hence, it is proposed that using minimally-processed flax slivers (or rovings), processed specifically for composites applications rather than textile applications, as reinforcements in an epoxy matrix is a good starting point for producing high-quality PFRPs. Furthermore, employing prepregging technology for composite manufacture would enable the production of high fibre content and thus high-performance PFRPs. In addition, plant fibre surface treatment is not entirely necessary to achieve high PFRP mechanical properties.

Table 3.7. Tensile properties of unidirectional (long bast fibre reinforced) PFRPs reported in literature.

		$Fibre \ volume \ fraction \ v_f$	Tensile modulus E _c	$Fibre \ tensile \ modulus^\dagger \ E_f$	Tensile strength σ_c	Fibre $tensile \\ strength^{\dagger} \\ \sigma_f$	
Unidirectional composite	Manufacturing technique	[%]	[GPa]	[GPa]	[MPa]	[MPa]	Source
Jute yarn/epoxy	Filament winding *	40	15	32	155	-	[53]
Jute sliver/polyester	Compression moulding	32	20	56	170	442	[22]
Hemp yarn/PET	Compression moulding	34	18	51	205	538	[17]
Flax yarn/epoxy	Prepregging	50	32	61	315	600	[10]
Flax roving/epoxy	Prepregging	48	37	73	377	751	[10]
Flax sliver/epoxy	Prepregging	42	40	90	378	860	[10]
Flax sliver/epoxy	Prepregging	48	32	63	268	505	[9]
Flax sliver/epoxy	RTM	42	35	79	280	710	[52]
Flax sliver/polyester	Compression moulding	35	14	37	210	496	[54]
Flax yarn/vinylester	RTM	37	24	60	248	-	[7]

[†] The fibre properties have been 'back-calculated' by the authors of the respective articles.

^{*} Typically, samples are compression/press moulded after filament winding.

3.3.2.3 Impact properties

Impact energy is typically dissipated by fibre and/or matrix fracture, debonding and fibre pull-out. Fibre pull-out dissipates more energy than fibre fracture [55]. Importantly, the former indicates weak interfacial properties, while the latter indicates good fibre/matrix adhesion [55]. The impact strength of the composite laminates is presented in Fig. 3.9. Noticeably, epoxy composites exhibit 10-30% lower impact strength than polyester composites. As improved fibre/matrix adhesion is known to affect impact strength adversely [55], this indicates that plant fibres are more compatible with epoxy than polyester. This is consistent with the fracture surfaces of impact-tested specimens, where epoxy composites exhibit considerably less fibre pull-out than polyester composites, and the fact that the former display higher 'apparent' interlaminar shear strength (Fig. 3.6).

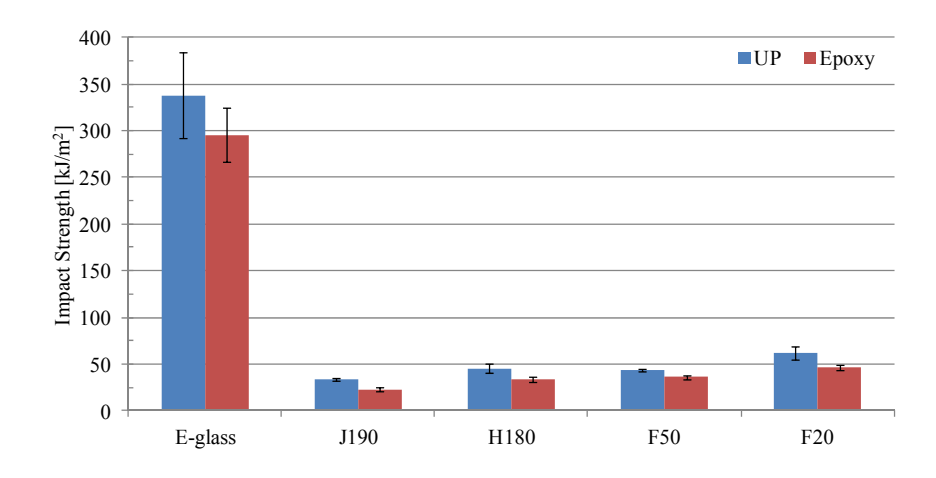


Fig. 3.9. Impact strength of PFRPs compared to E-glass composites.

The impact properties of PFRPs compare poorly to GFRPs, even when compared in terms of specific impact strength. Where unidirectional GFRPs have impact strengths of 300-350 kJ/m², unidirectional PFRPs have 5 to 10 times lower impact strengths of 30-60 kJ/m². Typically, short random PFRPs have impact strengths in the range of 10-25 kJ/m² [20, 55].

It is generally accepted that the toughness of a composite is mainly dependent on the fibre stress-strain behaviour, as well as the interfacial bond strength [55, 56]. E-glass

fibres are stronger than bast fibres with similar failure strain, and hence they may impart high work to fracture on the composites. In addition, while E-glass fibres are isotropic due to a 3-dimensional network of SiO₂, plant fibres are anisotropic with oriented cellulose microfibrils. Furthermore, synthetic E-glass has uniform properties, while natural fibres have non-uniform properties, particularly due to the presence of various defects (such as kinks). These are the prime reasons for the poorer impact properties of PFRPs [56-58].

Amongst PFRPs, F20 composites have best impact properties. It is interesting to note that impact strength of PFRPs reduces with increasing yarn twist level (Fig. 3.9). It is proposed that yarn construction and composite porosity are key factors in PFRP impact properties. High-twist yarn PFRPs have large intra-yarn voids, which can act as stress-raisers and likely sites for crack propagation. Furthermore, fibres are well-separated ('defibrillated') in low-twist yarn PFRPs, particularly flax F20, while fibre distribution is inhomogeneous in high-twist yarn PFRPs, resulting in resin rich zones (Fig. 3.3). Essentially, the crack path is likely to be more complex in low-twist yarn PFRPs, resulting in a higher work to fracture.

The inferior impact properties of PFRPs can be used as indicators of possible applications. Alternatively, the impact properties can be improved by *i*) using hybrid reinforcements (*e.g.* flax/E-glass or flax/coir) [57, 59], or *ii*) employing alternate textile architectures (*e.g.* mutliaxial non-wovens/wovens) and ply stacking sequence [4, 59]. In a hybrid reinforcement, fibres with good impact resistance (such as, E-glass or plant fibre with high microfibril angles such as coir and sisal) can be combined with bast fibres to produce improved impact properties ([57, 59] and references therein).

3.4 Conclusions

This study on the mechanical properties of aligned plant yarn reinforced thermoset composites has several key conclusions. Plant fibre reinforcements in the forms of yarns/rovings offer high length efficiency factors to the resulting composite due to low critical fibre lengths and high fibre aspect ratios. The manufactured PFRPs are well-impregnated and have low void content and consistent mechanical properties.

Considering the effect of thermoset matrix type, it is found that epoxies form a stronger interface with plant fibres than polyesters do. However, the effects of matrix type on longitudinal tensile properties of yarn reinforced PFRPs are inconclusive.

PFRPs consistently have lower fibre volume fractions than GFRPs, due to the low packing-ability of plant fibre preforms. Apart from the expected (30-40%) lower density of PFRPs, they have 20-30% lower interlaminar shear strength, 5-10 times lower impact strength, 60-80% lower tensile strength and 30-60% lower tensile stiffness than GFRPs. Hence, GFRPs clearly outperform PFRPs in terms of absolute mechanical properties. However, PFRPs have comparable specific stiffness performance to GFRPs.

Amongst the various yarn reinforced PFRPs studied, composites reinforced with flax rovings exhibit exceptional properties, with a back-calculated fibre tensile modulus in the range of 65-75 GPa (comparable to that of E-glass) and fibre tensile strength of about 800 MPa (half that of E-glass). These properties are achieved without using any active fibre surface treatment. Not only the fibre type, but yarn construction (twist level and packing fraction) and fibre/yarn quality are also found to have a significant impact on the mechanical properties of the resulting composite.

It is proposed that using minimally-processed flax rovings/slivers, processed specifically for composites rather than textile applications, as reinforcements in an epoxy matrix is a good starting point for producing high-quality PFRPs. Furthermore, fibre surface modification, for improved fibre/matrix adhesion, is not thought to be compulsory in achieving high mechanical properties.

3.5 REFERENCES

- 1. Lewin M. *Handbook of fiber chemistry*. Third ed, 2007. Boca Raton: CRC Press LLC
- 2. Carus M. Bio-composites: Technologies, applications and markets, in 4th International Conference on Sustainable Materials, Polymers and Composites. 6-7 July 2011. Birmingham, UK.
- 3. Aly M, Goda IGM, Hassan GA. Experimental investigation of the dynamic characteristics of laminated composite beams. *International Journal of Mechanical & Mechatronics*, 2011, 10(3): p. 59-68.
- 4. Harris B. *Engineering composite materials*, 1999. London: The Institute of Materials.

- 5. Cichocki JF, Thomason JL. Thermoelastic anisotropy of a natural fiber. *Composites Science and Technology*, 2002, 62: p. 669-678.
- 6. Madsen B. *Properties of plant fibre yarn polymer composites An experimental study*. PhD, 2004. Technical University of Denmark: Lyngby, Denmark.
- 7. Goutianos S, Peijs T, Nystrom B, Skrifvars M. Development of flax fibre based textile reinforcements for composite applications. *Applied Composite Materials*, 2006, 13(4): p. 199-215.
- 8. Madsen B, Thygesen A, Lilholt H. Plant fibre composites Porosity and volumetric interaction. *Composites Science and Technology*, 2007, 67: p. 1584-1600.
- 9. Weyenberg I, Chitruong T, Vangrimde B, Verpoest I. Improving the properties of UD flax fibre reinforced composites by applying an alkaline fibre treatment. *Composites Part A: Applied Science and Manufacturing*, 2006, 37: p. 1368-1376.
- 10. Baets J, Plastria D, Ivens J, Verpoest I. Determination of the optimal flax fibre preparation for use in UD-epoxy composites, in *4th International Conference on Sustainable Materials, Polymers and Composites*. 6-7 July 2011. Birmingham, UK.
- 11. Boey F, Lye SW. Void reduction in autoclave processing of thermoset composites: Part 1: High pressure effects on void reduction. *Composites*, 1992, 23(4): p. 261-265.
- 12. Anderson J, Altan MC. Properties of composite cylinders fabricated by bladder assisted composite manufacturing. *Journal of Engineering Materials and Technology*, 2012, 134: p. 1-7.
- 13. Ghiorse S. Effect of void content on the mechanical properties of carbon/epoxy laminates, in SAMPE Quarterly, 1993. p. 54-59.
- 14. Madsen B, Thygesen, A, Liholt, H. Plant fibre composites Porosity and stiffness. *Composites Science and Technology*, 2009, 69: p. 1057-1069.
- 15. Madsen B, Lilholt H. Physical and mechanical properties of unidirectional plant fibre composites an evaluation of the influence of porosity. *Composites Science and Technology*, 2003, 63: p. 1265-1272.
- 16. Zhang L, Miao M. Commingled natural fibre/polypropylene wrap spun yarns for structured thermoplastic composites. *Composites Science and Technology*, 2010, 70: p. 130-135.
- 17. Madsen B, Hoffmeyer P, Lilholt H. Hemp yarn reinforced composites II. Tensile properties. *Composites Part A: Applied Science and Manufacturing*, 2007, 38: p. 2204-2215.
- 18. Lee B, Kim HJ, Yu WR. Fabrication of long and discontinuous natural fiber reinforced polypropylene biocomposites and their mechanical properties. *Fibers and Polymers*, 2009, 10(1): p. 83-90.
- 19. Zarate C, Aranguren MI, Reboredo MM. Influence of fiber volume fraction and aspect ratio in resol-sisal composites. *Journal of Applied Polymer Science*, 2003, 89: p. 2714-2722.
- 20. Rodríguez E, Petrucci R, Puglia D, Kenny JM, Vazquez A. Characterization of composites based on natural and glass fibers obtained by vacuum infusion. *Journal of Composite Materials*, 2005, 39(5): p. 265-282.
- 21. Oksman K, Wallstrom L, Berglund LA, Filho RDT. Morphology and mechanical properties of unidirectional sisal-epoxy composites. *Journal of Applied Polymer Science*, 2002, 84: p. 2358-2365.
- 22. Roe P, Ansell MP. Jute-reinforced polyester composites. *Journal of Materials Science*, 1985, 20: p. 4015-4020.
- Goutianos S, Peijs T. The optimisation of flax fibre yarns for the development of high-performance natural fibre composites. *Advanced Composites Letters*, 2003, 12(6): p. 237-241.

- 24. Baley C. Analysis of the flax fibres tensile behaviour and analysis of the tensile stiffness increase. *Composites Part A: Applied Science and Manufacturing*, 2002, 33: p. 939-948.
- 25. Virk A, Hall W, Summerscales J. Tensile properties of jute fibres. *Materials Science and Technology*, 2009, 25(10): p. 1289-1295.
- 26. Thygesen A. Properties of hemp fibre polymer composites An optimisation of fibre properties using novel defibration methods and fibre characterisation. PhD, 2006. The Royal Agricultural and Veterinary University of Denmark: Roskilde, Denmark.
- 27. Lilholt H, Bjerre AB. Composites based on jute-fibres and polypropylene matrix, their fabrication and characterization, in *18th Risø international symposium on materials science. Polymeric composites expanding the limits.* 1997. Roskilde, Denmark: Risø National Laboratory.
- 28. Baley C, Perrot Y, Busnel F, Guezenoc H, Davies P. Transverse tensile behaviour of unidirectional plies reinforced with flax fibres. *Materials Letters*, 2006, 60: p. 2984-2987.
- 29. Naik N, Singh MN. Twisted Impregnated Yarns: Shear strength. *Journal of the Textile Institute*, 2001, 92(2): p. 164-183.
- 30. Fu S, Lauke B, Mader E, Yue CY, Hu X. Tensile properties of short-glass-fiber- and short-carbon-fiber-reinforced polypropylene composites. *Composites Part A: Applied Science and Manufacturing*, 2007, 31: p. 1117-1125.
- 31. Placet V, Trivaudey F, Cisse O, Gucheret-Retel V, Boubakar ML. Diameter dependence of the apparent tensile modulus of hemp fibres: A morphological, structural or ultrastructural effect? *Composites Part A: Applied Science and Manufacturing*, 2012, 43(2): p. 275-287.
- 32. Charlet K, Jernot JP, Moussa G, Baley C, Bizet L, Breard J. Morphology and mechanical behaviour of a natural composite: the flax fiber, in *16th International Conference on Composite Materials (ICCM-16)*. 2007. Kyoto, Japan.
- 33. Awal A, Cescutti G, Ghosh SB, Mussig J. Interfacial studies of natural fibre/polypropylene composites using single fibre fragmentation test (SFFT). *Composites Part A: Applied Science and Manufacturing*, 2011, 42: p. 50-56.
- 34. Garkhail S, Heijenrath RWH, Peijs T. Mechanical properties of natural-fibre-matreinforced thermoplastics based on flax fibres and polypropylene. *Applied Composite Materials*, 2000, 7: p. 351-372.
- 35. Bos H. *The potential of flax fibres as reinforcement for composite materials*. PhD, 2004. Technische Universiteit Eindhoven: Eindhoven, Netherlands.
- 36. Mwaikambo L, Tucker N, Clark AJ. Mechanical properties of hemp-fibre-reinforced euphorbia composites. *Macromolecular Materials and Engineering*, 2007, 292: p. 993-1000.
- 37. Bos H, Mussig J, van den Oever MJA. Mechanical properties of short-flax-fibre reinforced compounds. *Composites Part A: Applied Science and Manufacturing*, 2006, 37: p. 1591-1604.
- 38. Sawpan M, Pickering KL, Fernyhough A. Analysis of mechanical properties of hemp fibre reinforced unsaturated polyester composites. *Journal of Composite Materials*, 2012, (In Press). doi:10.1177/0021998312449028.
- 39. Vallejos M, Espinach FX, Julián F, Torres LI, Vilaseca F, Mutjé P. Micromechanics of hemp strands in polypropylene composites. *Composites Science and Technology*, 2012, 72: p. 1209-1213.
- 40. Weyenberg I, Ivens J, Coster A, Kino B, Baetens E, Verpoest I. Influence of processing and chemical treatment of flax fibres on their composites. *Composites Science and Technology*, 2003, 63: p. 1241-1246.
- 41. Franck R, ed. Bast and other plant fibres. 2005. CRC Press LLC: Boca Raton.

- 42. Virk A, Hall W, Summerscales J. Modulus and strength prediction for natural fibre composites. *Materials Science and Technology*, 2012, 28(7): p. 864-871.
- 43. Cox H. The elasticity and strength of paper and other fibrous materials. *British Journal of Applied Physics*, 1952, 3: p. 72-79.
- 44. Kelly A, Tyson WR. Tensile properties of fibre-reinforced metals: Copper/tungsten and copper/molybdenum. *Journal of the Mechanics and Physics of Solids*, 1965, 13(6): p. 329-350.
- 45. Joffe R, Wallstrom L, Berglund LA. Natural fibre composites based on flax matrix effects, in *International Scientific Colloquium Modelling for Saving Resources*. 2001. Riga, Latvia.
- 46. Ashby M. *Materials selection in mechanical design*, 1992. Oxford, UK: Pergamon Press.
- 47. McLaughlin E, Tait RA. Fracture mechanism of plant fibres. *Journal of Materials Science*, 1980, 15: p. 89-95.
- 48. Mukherjee P, Satyanarayana KG. An empirical evaluation of structure-property relationships in natural fibres and their fracture behaviour. *Journal of Materials Science*, 1986, 21: p. 4162-4168.
- 49. Madsen B, Mehmood S, Aslan M. Variability in properties of natural fibres, in *NATEX Workshop*. 2012. Chesterfield, UK.
- 50. Hanninen T, Thygesen A, Mehmood S, Madsen B, Hughes M. Mechanical processing of bast fibres: The occurrence of damage and its effect on fibre structure. *Industrial Crops and Products*, 2012, 39: p. 7-11.
- 51. Pickering K, ed. *Properties and performance of natural-fibre composites*. 2008. CRC Press LLC: Boca Raton.
- 52. Oksman K. High quality flax fibre composites manufactured by the resin transfer moulding process. *Journal of Reinforced Plastics and Composites*, 2001, 20(7): p. 621-627.
- 53. Gassan J, Bledzki AK. Possibilities for improving the mechanical properties of jute/epoxy composites by alkali treatment of fibres. *Composites Science and Technology*, 1999, 59: p. 1303-1309.
- 54. Charlet K, Jernot JP, Gomina M, Bizet L, Bréard J. Mechanical properties of flax fibers and of the derived unidirectional composites. *Journal of Composite Materials*, 2010, 44(24): p. 2887-2896.
- 55. Wambua P, Ivens J, Verpoest I. Natural fibres: can they replace glass in fibre reinforced plastics? *Composites Science and Technology*, 2003, 63: p. 1259-1264.
- 56. Pavithran C, Mukherjee PS, Brahmakumar M, Damodaran AD. Impact properties of natural fibre composites. *Journal of Materials Science Letters*, 1987, 6: p. 882-884.
- 57. Santulli C. Impact properties of glass/plant fibre hybrid laminates. *Journal of Materials Science*, 2007, 42: p. 3699-3707.
- 58. Yuanjian T, Isaac, DH. Impact and fatigue behaviour of hemp fibre composites. *Composites Science and Technology*, 2007, 67: p. 3300-3307.
- 59. Nunna S, Chandra PR, Shrivastava S, Jalan AK. A review on mechanical behavior of natural fiber based hybrid composites. *Journal of Reinforced Plastics and Composites*, 2012, 31: p. 759-769.